Modeling Dermatome Selectivity of Single- and Multiple-Current Source Spinal Cord Stimulation Systems

Xiaoyi Min, Alexander R. Kent, Stuart P. Rosenberg and Timothy A. Fayram

***Abstract*—A recently published computational modeling study of spinal cord stimulation (SCS) predicted that a multiple current source (MCS) system could generate a greater number of central points of stimulation in the dorsal column (DC) than a single current source (1CS) system. However, the clinical relevance of this finding has not been established. The objective of this work was to compare the dermatomal zone selectivity of MCS and 1CS systems. A finite element method (FEM) model was built with a representation of the spinal cord anatomy and a 2×8 paddle electrode array. Using a contact configuration with two aligned tripoles, the FEM model was used to solve for DC field potentials across incremental changes in current between the two cathodes, modeling the MCS and 1CS systems. The activation regions within the DC were determined by coupling the FEM output to a biophysical nerve fiber model, and coverage was mapped to dermatomal zones. Results showed marginal differences in activated dermatomal zones between 1CS and MCS systems. This indicates that a MCS system may not provide incremental therapeutic benefit as suggested in prior analysis.**

I. Introduction

Spinal cord stimulation (SCS) is an effective therapy for the management of chronic pain. Components of SCS systems generally include an implantable pulse generator (IPG) connected to one or more stimulation leads placed in the epidural space of the spinal column. Delivery of electrical current through the leads generates field potentials in the spinal cord, and supra-threshold potentials can produce nerve fiber activation. It is thought that SCS therapy is based on the "gate-control theory," in which electrical activation of large, myelinated mechanoreceptor afferents (Aβ fibers) indirectly modulates the transmission of painful information from small, unmyelinated afferents (C fibers) within the dorsal horn [1]. Successful delivery of SCS generates paresthesia that completely and consistently covers the pain originating from targeted body area(s), yet does not cause uncomfortable sensations. This paresthesia is elicited by activation of fibers in the dorsal root (DR) or fiber tracts in the dorsal column (DC), which are hereafter referred to as "dermatomal zones." Electrical stimulation of the DC typically causes paresthesia in a number of dermatomes around the level of the stimulating cathode.

Computational modeling has been used to study the effects of SCS and to guide system design. This tool can be used to calculate neuronal activation within the spinal cord across a range of parameters, and thereby assist in selection of electrode combinations and stimulation settings, which becomes more complex as the number of contacts on leads increases.

Modern SCS systems have been designed with single and multiple stimulation sources. Recently published work [2] using computer simulations of SCS predicted that a multiple current source (MCS) system could generate a greater number of central points of activation within the DC compared to a single current source (1CS) system. MCS systems can deliver current to each cathode in a controlled manner, with as fine as 1% increments in amplitude, and modeling results suggest a corresponding central point medial-lateral resolution of 0.02 mm. Conversely, a 1CS systems deliver current to one or more cathodes, but cannot make incremental adjustments in the amount delivered to each cathode. The clinical relevance of the number and resolution of central points on paresthesia-pain coverage in patients has not been established. It may be more relevant to clinical outcomes to compare the overall activation region within the DC and to study the corresponding dermatome areas affected. The objective of this analysis was to compare the dermatomal zone selectivity of 1CS and MCS systems.

II. Methods

We developed a computer model for simulating the effect of SCS on DC fibers in the spinal cord, using an approach similar to that described by Holsheimer and colleagues at the University of Twente [3]. The model consisted of two stages: 1) a three-dimensional volume conductor model representing the anatomical and conductive properties of the SC, and 2) a biophysical model of mammalian, myelinated nerve fibers. The electrical fields produced by stimulation with the SCS electrode were computed with the volume conductor model and coupled to the nerve fiber model to determine which fibers in the DC were activated.

Research sponsored by St. Jude Medical, Inc.

Xiaoyi Min is with St. Jude Medical, Sylmar, CA 91342 USA (e-mail: xmin@sjm.com).

Alexander R. Kent is with St. Jude Medical, Sunnyvale, CA 94085 USA (e-mail: akent02@sjm.com).

Stuart P. Rosenberg is with St. Jude Medical, Sylmar, CA 91342 USA (e-mail: srosenberg@sjm.com).

Tim A. Fayram is with St. Jude Medical, Sunnyvale, CA 94085 USA (e-mail: tfayram@sjm.com).

978-1-4244-7929-0/14/$26.00 ©2014 IEEE

A. *Volume Conductor Model*

A volume conductor model was constructed using the finite element method (FEM) in ANSYS Maxwell 3D to calculate the electric fields generated during SCS (Fig. 1). Representations of DC and other white and grey matter, cerebrospinal fluid (CSF), epidural fat, and vertebral bone at T7-T10 vertebral levels were based on the geometries of the University of Twente low thoracic model [3]. The conductivity properties of the tissues were obtained from [4] and are summarized in Table 1. The choice of CSF thickness (3.2 mm) was based on MRI images from 26 normal human subjects at corresponding vertebral levels [5].

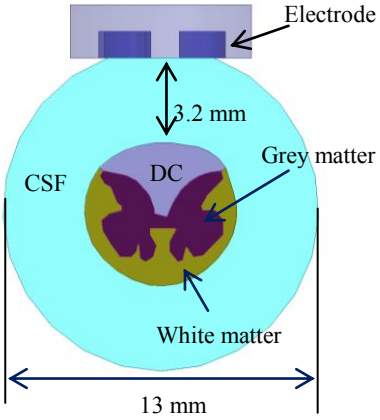

Figure 1. Transverse 2D cross-section of spinal cord anatomy, including dorsal column (DC) and other white matter tracts, grey matter, and cerebro-spinal fluid (CSF), as well as the SCS paddle array (body and electrode contacts), in the FEM model.

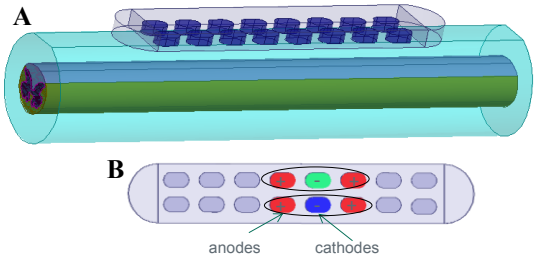

Figure 2. (A) 3D representation of the FEM model geometry, including spinal cord and 2×8 paddle array in the epidural space. (B) Contact configuration using two aligned tripoles (circled), showing locations of anodes (red) and cathodes (blue and green).

The volume conductor model included a 2×8 paddle electrode array to simulate effects of varying current in two side-by-side cathodes. The electrode contacts were 1.8 mm in width by 3 mm in length with 1.2 mm longitudinal and 1.1 mm lateral edge-to-edge spacing, and the paddle was placed symmetrically in the dorsal epidural space, as shown in Figs. 1 and 2A. To generate an electric field, constant-current boundary conditions were imposed at activated contacts. The MCS system was modeled by using a configuration with two aligned tripoles and incremental current changes between the two cathodes (Fig. 2B). The total current was split into the two cathodes at specified current ratios for five settings (left:right cathode split: 100%:0%; 87.5%:12.5%; 75%:25%; 62.5%:37.5%, and 50%:50%). The area of activation in the DC would be approximately "mirrored" with reversal of left:right cathode split (e.g. 100%:0% versus 0%:100%). For the 1CS system, the current was delivered either all to the left cathode or split approximately equally between both cathodes. The field potentials within the DC were coupled to the biophysical nerve fiber model to determine the corresponding activation regions.

Table 1. Tissue conductivity properties in the FEM model.

Material	Tissue Conductivity (S/m)
Grey Matter	0.25
White Matter (Longitudinal)	0.72
White Matter (Transverse)	0.083
CSF	1.67
Epidural Fat	0.05
Vertebral Bone	0.025

B. *Biophysical Model of Myelinated Nerve Fibers*

A cable-based biophysical nerve fiber model was built in NEURON v7.3 and used to determine the response of neurons in the DC to SCS. Specifically, we implemented the Sweeney model of mammalian, myelinated nerve fibers [6, 7]. This model represents nodes of Ranvier with transmembrane sodium ion and leakage currents in parallel with membrane capacitance. The nodes are connected to adjacent myelinated internodal segments via intracellular conductance. The myelin sheath is considered perfectly insulating (no current flow). The internodal diameter and length were 12 µm and 1.2 mm respectively, whereas node diameter and length were 7.2 µm and 1.5 µm, respectively [8, 9]. The entire DC was populated with representative nerve fibers using a grid arrangement in the transverse plane, with 50 µm grid resolution (2520 fibers total).

C. *Coupling the Volume Conductor and Biophysical Models to Calculate Dorsal Column Activation*

A single cathodic pulse (step waveform of 100 µs duration) was delivered to the nerve fibers. Potentials calculated with the volume conductor model were interpolated at the locations of the nodes of Ranvier of all fibers and applied to the cellular model as an extracellular field. Since the bulk conductivity of the model was linear, the extracellular potentials generated by different amplitudes were scaled versions of the original FEM solution. The stimulus pulse was delivered within the cellular model after a 0.1 ms delay to allow for initialization to steady state, and the total simulation time for observing the response of a given nerve fiber to stimulation was 2 ms.

Nerve fiber activation was detected by monitoring the transmembrane potential (V_M) at the middle node of each fiber, with $V_M \geq$ -20 mV indicating action potential generation [10]. The DC stimulation threshold was defined as the stimulation amplitude required to activate one fiber in the DC. Subsequently, the discomfort threshold was calculated as the stimulation threshold multiplied by a factor of 1.4 [11], and corresponds to activation of small fibers in the DC or fibers in the DR [3, 4]. The range between the DC

and discomfort thresholds was used to set the stimulation amplitudes for testing.

The activation regions were defined by determining which nerve fibers in the DC were excited under a given set of stimulation conditions. Axon coverage was further mapped to dermatomal fiber tracts by an established template [12], shown in Figure 3.

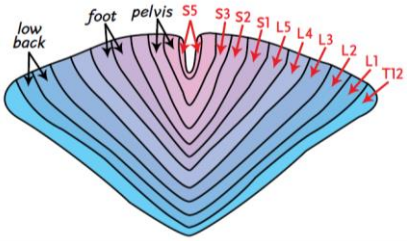

Figure 3. A template of dermatomal zones at the T11 segment. Used with permission from [12].

III. Results

A. Calculation of Stimulation Thresholds

Average stimulation thresholds in the DC were 2.65 ± 0.11 mA and discomfort thresholds were 3.70 ± 0.16 mA for the current split ratios with the MCS system (Table 2). Therefore, stimulation amplitudes at the contacts were set within this range to 3.0 mA, 3.2 mA, or 3.4 mA, and the corresponding activation regions in DC were calculated in Section B.

B. Activation Regions

Activation regions were calculated for 1CS and MCS current split ratios at the different stimulation amplitudes (Fig. 4). As current split ratios were changed with fixed total current amplitude, activation regions were largely overlapping, with only small shifts in activation area at the borders.

Table 2. DC stimulation thresholds and discomfort thresholds, defined as 140% of DC threshold, at different current split ratios with the MCS system.

Current Split Ratio	DC Threshold (mA)	Discomfort Threshold (mA)
100%:0%	2.47	3.46
87.5%:12.5%	2.60	3.64
75%:25%	2.68	3.75
62.5%:32.5%	2.73	3.82
50%:50%	2.75	3.85

C. Dermatomal Zones

The DC activation regions were mapped into dermatomal zones as shown in Table 3, with grey level representing current amplitude at 3.0 mA, (■) 3.2 mA (■), and 3.4 mA (■). For both MCS and 1CS systems with 100% of the current to the left cathode and 3 mA total current amplitude,

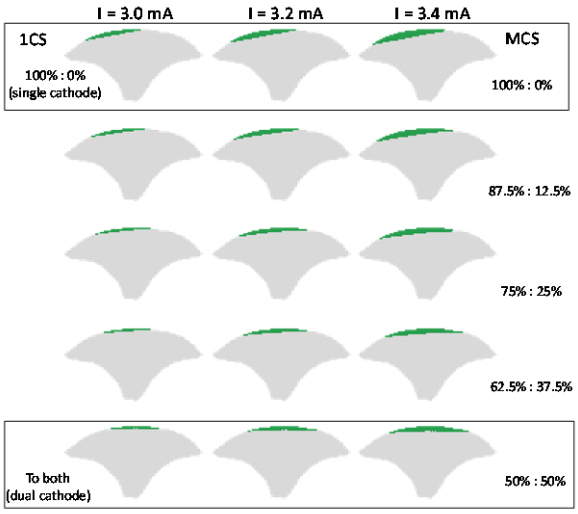

Figure 4. DC activation regions (green fill) at different stimulation current inputs. The plots are arranged along each row with five ratios of current split, and along each column with three stimulation current amplitudes (3.0 mA, 3.2 mA, and 3.4 mA).

the covered dermatomal zones were left L3-L5, left S1-S5 and right S4-5. When injecting 3 mA between right and left cathodes with a 50%:50% split in 1CS or MCS systems, dermatomal zones covered were left S1-S5, and right S1-S5. Between the 100%:0% and 50%:50% levels, incrementally splitting the current between the cathodes of the MCS system in 12.5% steps showed a maximum of one shift in dermatomal zone coverage on the left or right DC, consistent across all stimulation amplitudes tested (3.0 mA, 3.2 mA, or 3.4 mA). Thus, there were widely overlapping dermatomal zones with variation in current split ratios with the MCS system.

Table 3. Dermatomal zones mapped from activation regions for MCS (all rows) and 1CS (only 100%:0% and 50%:50% rows) systems. Mapped zones extend from left to right L1. Activation is shown for the three tested stimulation current amplitudes: 3.0 mA (■), and additional dermatomal activation with increasing of amplitude to 3.2 mA (■) and then to 3.4 mA (■). In some cases, dermatomal zone activation was unchanged on the left or right side with an incremental change in current split ratio (e.g., right zones unchanged with 75%:25% split and increase from 3.2 to 3.4 mA).

Current Split Ratio	Left Zones										Right Zones									
	L1	L2	L3	L4	L5	S1	S2	S3	S4	S5	S5	S4	S3	S2	S1	L5	L4	L3	L2	L1
100%:0%		■	■	■	■	■	■	■	■	■	■	■	■	■						
87.5%:12.5%			■	■	■	■	■	■	■	■	■	■	■	■	■					
75%:25%			■	■	■	■	■	■	■	■	■	■	■	■	■					
62.5%:37.5%				■	■	■	■	■	■	■	■	■	■	■	■	■				
50%:50%					■	■	■	■	■	■	■	■	■	■	■	■	■			

Increasing stimulation current amplitude from 3.0 mA to 3.2 or 3.4 mA broadened the dermatomal zone coverage (Table 3). Consequently, the incremental changes in coverage achieved by the MCS system could also be obtained using the 1CS system with adjustment in the current amplitude. More specifically, varying total current from 3.0 mA to 3.4 mA in 0.1 mA increments with a single cathode in the 1CS system extended the dermatomal zones to the right side smoothly by a maximum step of one dermatomal zone (Table 4).

Table 4: Dermatomal zones mapped from activation regions for the 1CS system with a current split ratio of 100%:0% (single cathode) and total stimulation current varied from 3.0 to 3.4 mA.

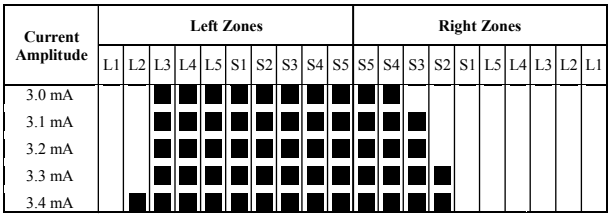

IV. Discussion

The wide overlap of activation regions across current split ratios with the MCS system suggests that using central points of activation as a proxy for dermatomal zone coverage may not be clinically relevant. This is because activation of nerve fibers drives therapeutic effect, and the central point is not fully representative of the mass of activated DC fibers. In addition, incrementally splitting the current between the cathodes of the MCS system showed that changes in dermatomal zone coverage occurred with a minimum step size of 12.5%, so smaller steps were unnecessary and did not lead to any clinically detectable changes. Importantly, incremental changes in dermatomal coverage could likewise be obtained with a 1CS system by adjusting total current amplitude. This small effect of current steering with the MCS system could be due at least in part to current shunting by the CSF.

Alternatively, use of a SCS paddle lead with a large number of stimulation contacts allows for flexibility in contact configuration and achieving of gapless coverage in the DC with a 1CS system [13].

Finally, using the 2×8 paddle array, it was difficult to activate dermatomes corresponding to the lower back (L1 and L2), which are located in the lateral region of the DC. A high stimulation current amplitude, close to the discomfort threshold, was required for activation of L2, with substantial concomitant activation of other dermatomes.

V. Limitations

The model did not account for patient variation in SC anatomy or variation in dermatome topography within the DC. In particular, the thickness and location of the spinal column within the CSF could be highly variable between patients. This could impact field potentials generated by SCS within the DC due current shunting by the CSF, which has a higher conductivity compared to surrounding tissue. Additionally, dermatomal zone topography is expected to vary across the vertebral levels represented in the FEM model, but our mapping did not accommodate this variability. Electrode locations may vary within patients, such as with changes in posture or following migration, as well as across patients, but this was not factored into the model. Finally, we used a fixed nerve fiber diameter, rather than a distribution of nerve fiber diameters, as expected in the DC [12].

VI. Conclusion

Computer modeling shows a small difference in activated dermatomes between single- and multiple-current source SCS systems. We contend that the higher resolution of central points provided by a multiple current-source system may have little impact on dermatomal zone coverage beyond what can be achieved by adjustments in stimulation amplitude. It is unclear if there would be any incremental therapeutic benefit of a multiple current-source system.

References

[1] R. Melzack and P. D. Wall, "Pain mechanisms: a new theory," *Science*, vol. 150, no. 3699, pp. 971-979, Nov. 1965.

[2] D. Lee, E. Gillespie, K. Bradley, "Dorsal column steerability with dual parallel leads using dedicated power sources: a computational model," *J. Vis. Exp.*, vol. 48, pp. 2443, Feb. 2011.

[3] J. Holsheimer and W. A. Wesselink, "Effect of anode-cathode configuration on paresthesia coverage in spinal cord stimulation," *Neurosurgery,* vol. 41, no. 3, pp. 654-659, Sep. 1997.

[4] J. Holsheimer and W. A. Wesselink, "Optimum electrode geometry for spinal cord stimulation: the narrow bipole and tripole," *Med. Biol. Eng. Comput.,* vol. 35, no. 5, pp. 493-497, 1997.

[5] J. Holsheimer and G. Barolat, "Spinal geometry and paresthesia coverage in spinal cord stimulation," Neuromodulation. vol. 1, no. 3, pp. 129-136, 1998.

[6] J. D. Sweeney, J. T. Mortimer, and D. Durand, "Modeling of mammalian myelinated nerve for functional neuromuscular electrostimulation," *IEEE 9th Annu. Conf. Eng. Med. Biol. Soc.*, pp. 1577-1578, 1987.

[7] C. C. McIntyre and W. M. Grill, "Sensitivity analysis of a model of mammalian neural membrane," *Biol. Cybern.,* vol. 79, no. 1, pp. 29-37, Jul. 1998.

[8] D. Lee, B. Hershey, K. Bradley, and T. Yearwood, "Predicted effects of pulse width programming in spinal cord stimulation: a mathematical modeling study," *Med. Biol. Eng. Comput.*, 49(7): 765-774, Jul. 2011.

[9] E. N. Warman, W. M. Grill, and D. Durand, "Modeling the effects of electric fields on nerve fibers: determination of excitation thresholds," *IEEE Trans. Biomed. Eng.*, vol. 39, no. 12, Dec. 1992.

[10] A. R. Kent and W. M. Grill. "Model-based analysis and design of nerve cuff electrodes for restoration of bladder function by selective stimulation of the pudendal nerve," *J. Neural Eng.*, vol. 10, no. 3, pp. 1-15, Apr. 2013.

[11] M. A. Moffitt, D. C. Lee, and K. Bradley, "Spinal Cord Stimulation: Engineering Approaches to Clinical and Physiological Challenges," in Implantable Neural Prostheses 1:devices and applications, D.D. Zhou, E. Greenbaum, Eds. Springer Science + Business Media, 2009, pp. 155–194.

[12] H. K. Feirabend, H. Choufoer, S. Ploeger, J. Holsheimer, and J. D. van Gool, "Morphometry of human superficial dorsal and dorsolateral column fibres: significance to spinal cord stimulation," *Brain,* vol. 125 (pt. 5), pp. 1137-1149, May 2002.

[13] A. R. Kent, X. Min, S. P. Rosenberg, and T. A. Fayram, "Computational Modeling Analysis of a Spinal Cord Stimulation Paddle Lead Reveals Broad, Gapless Dermatomal Coverage," *IEEE 36th Annu. Conf. Eng. Med. Biol. Soc.,* submitted for publication.